Experimental Observation of Anharmonic Coupling of the Heme-Doming and Iron−Ligand Out-of-Plane Vibrational Modes Confirmed by Density Functional Theory

Stefan Franzen,*,† Klaus Fritsch,‡ and Scott H. Brewer†

Department of Chemistry, North Carolina State University, Raleigh, North Carolina 27695, and Los Alamos National Laboratory, Los Alamos, New Mexico 87545

Received: May 15, 2002; In Final Form: August 7, 2002

In the deoxy ferrous state of histidine-ligated heme proteins, the iron−histidine band (ν_{Fe-His}) has been assigned as a stretching mode that involves a two-body motion involving the iron and histidine combined with a minor amount of heme doming. An analogous Raman band, ν_{Fe-L} has been observed in the proximal cavity mutant of H93G myoglobin where the Raman band of a series of nonnative axial ligands, L, can be compared. The H93G mutant of myoglobin consists of substitution of the proximal histidine, H93, by glycine. This replacement abolishes the sole covalent connection between the globin and the heme iron and creates a cavity that can be occupied by exogenous ligands, L, by dialysis. In the present study, the iron−axial-ligand out-of-plane vibration, ν_{Fe-L}, for a series deoxy ferrous heme-iron adducts H93G(L) has been measured as a function of temperature, where L = imidazole (Im), 4-methyl imidazole (4-Me Im), 2-methyl imidazole (2-Me Im), 1-methyl imidazole (1-Me Im), 4-bromo imidazole (4-Br Im), and 2,4-dimethyl imidazaole (2,4-diMe Im). Density functional theory calculations show that anharmonic coupling between low wavenumber heme-doming and iron−ligand out-of-plane modes can account for the calculated ν_{Fe-L} frequency shifts. These calculations parallel the experimental observed trends for temperature-dependent Raman spectra for all of the adducts except H93G-(1-Me Im).

Introduction

Iron serves as the binding site for oxygen in globins and the active site for O−O bond scission in peroxidases and oxidases. A histidine is the sole covalent connection between the protein and the heme iron active site of peroxidases, oxidases, and globins. Resonant Raman spectra of heme proteins have shown that a band in the region 200−250 cm^{-1} that involves motion of both the iron and histidine[1] is also sensitive to protein conformation[2,3] and pH.[4] The frequency of the iron−histidine mode, ν_{Fe-His}, is correlated with binding strength in hemoglobin,[5,6] reactivity in peroxide,[7] and the state of ligation of the heme in cytochrome *c* oxidase.[8] The frequency differences in ν_{Fe-His} suggest that ligand−iron bonding is important for differences in reactivity among these heme proteins. However, comparisons among different proteins are based on the assumption that the vibrational mode is similar in nature in different proteins. If large differences in conformational coupling of the iron−histidine anharmonic coupling of this mode to other normal modes in the protein exist, then the significance of the frequency comparisons do not reflect differences in iron−histidine bonding alone.

The higher frequency of the iron−histidine vibrational mode in peroxidases ($\nu_{Fe-His} \approx 243-245$ cm^{-1}), when compared to globins, has been understood in terms of the stronger hydrogen bond between an aspartate and the imidazole N−H as opposed to the weak H bond between serine and the imidazole N−H in the globins.[7,9] The proposed correlation with the frequency of the ν_{Fe-His} mode suggests that the higher the frequency of this mode, the greater the electron density on the heme iron and, therefore, the greater the extent of activation of bound oxygen.[7] On the other hand, the lower frequency of ν_{Fe-His} observed in cytochrome *c* oxidase[10] may be due to weaker hydrogen bonding inferred from X-ray crystal data.[11] The functional importance of the lower frequency in cytochrome *c* oxidase is not well understood. The enzyme dehaloperoxidase from *Amphitrite Ornata* that has $\nu_{Fe-His} \approx 232$ cm^{-1} intermediate between a globin and a peroxidase has a structure that is consistent with a globin structure, but this frequency is suggestive of an ability to activate bound oxygen.[12] Guanylyl cyclase[13] has a still lower frequency of $\nu_{Fe-His} \approx 206$ cm^{-1} indicative of a labile histidine as required by the function of the protein in signal transduction. The origin of the frequency differences in these proteins appears to depend on the strength of the iron−histidine bonding rather than conformational coupling suggested for hemoglobin. However, the role played by strain is not known, and the interpretation of the bond strength−frequency correlation will depend on the magnitude of anharmonic coupling that is manifested in the temperature dependence of the ν_{Fe-His} Raman band.

Frequency shifts of the ν_{Fe-His} vibrational mode have been observed as a function of temperature in the deoxy state and as a function of time following ligand photolysis. Hemoglobin provides an example of time-dependent shifts in the frequency of ν_{Fe-His}. The difference in frequency between the R (high affinity) and T (low affinity) states in hemoglobin is characterized by a difference in the frequency of the ν_{Fe-His} Raman mode with $\nu_{Fe-His} \approx 224$ cm^{-1} in the R state (10 ns photoproduct) and $\nu_{Fe-His} \approx 216$ cm^{-1} in the T state (equilibrium). The frequency lowering has been interpreted in terms of a weakening of the iron−histidine bond in the T state relative to the R state. The frequency, ν_{Fe-His}, in hemoglobin and myoglobin is also temperature dependent.[6,14,15] Deoxy myoglobin exhibits an increase from $\nu_{Fe-His} \approx 217$ cm^{-1} [16] at ambient temperature to $\nu_{Fe-His} \approx 226$ cm^{-1} at 10 K (i.e., $\approx$3 cm^{-1}/100 K).[14] The increase in band frequency of ν_{Fe-His} in deoxy hemoglobin

* To whom correspondence should be addressed: Phone: (919)-515-8915. Fax: (919)-515-8909. E-mail: Stefan_Franzen@ncsu.edu.
† North Carolina State University.
‡ Los Alamos National Laboratory.

10.1021/jp0261197 CCC: $22.00
Published on Web 10/10/2002

shows an increase from $\nu_{Fe-His} \approx 216$ cm^{-1} at ambient temperature to $\nu_{Fe-His} \approx 224$ cm^{-1} at 10 K ($\approx$3 cm^{-1}/100 K).[6] Temperature-dependent shifts in the frequency of a vibrational mode have been ascribed to anharmonicity.[17] The comparison of frequency shifts due to conformation (time-dependence) and anharmonic coupling (temperature dependence) is considered in this study to ascertain whether these two observations are coupled.

The proximal cavity mutant of myoglobin H93G provides an excellent test of the effect of bonding on different axial ligands within the same protein. In this study, we compare a series of iron−axial-ligand adducts in the H93G mutant of myoglobin. The H93G mutant of myoglobin consists of substitution of the proximal histidine, H93, by glycine.[18,19] This replacement abolishes the sole covalent connection between the globin and the heme iron and creates a cavity that can be occupied by exogenous ligands by dialysis. The heme-iron adducts are analogous to heme model systems;[20−22] however, the adducts are surrounded by the globin. In the present study, the Raman spectra of the deoxy ferrous heme-iron adducts of a series of substituted imidazoles demonstrates a temperature dependence of the ν_{Fe-L} Raman band, where L is the axial ligand. Analysis within the harmonic approximation reveals that the axial ligand out-of-plane mode, ν_{Fe-L}, is an iron−axial-ligand stretching vibration (50−70% of the potential energy distribution or PED) with a minor contribution of the heme doming coordinate (50−30% of the PED).[23] The temperature-dependent resonant Raman data are compared with density functional theory (DFT) calculations. Although single mode or intrinsic anharmonicity does not play an important role in the temperature dependence, anharmonic mulitmode coupling between iron−axial out-of-plane motion (heme-doming) and the iron−ligand out-of-plane normal mode can account for the temperature-dependent shifts observed experimentally. The anharmonic-coupling hypothesis[17] is tested and confirmed in the present study.

Experimental Section

Samples of H93G myoglobin with different ligands were prepared by dialysis as discussed previously.[19] The samples were prepared in 50% glycerol/phosphate buffer mixtures (w/v). The deoxy form of myoglobin was prepared by dilution into deoxygenated buffer followed by reduction with excess dithionite. Solutions were placed in a NMR tube spinning cell at ambient temperature and on a gold-plated copper coldfinger under argon for low-temperature experiments.

Resonance Raman experiments were performed using a Coherent 590 dye laser (Stilbene-420 dye) pumped by the UV lines of a Coherent Innova 400 Ar^+ ion laser. The laser frequency was tuned to 430 nm and focused on the coldfinger at the tip of the expander unit of an Air Products liquid-helium-cooled refrigerator. Typical laser powers were 10−20 mW. The temperature was monitored by a calibrated thermocouple in intimate contact with the coldfinger. Scattered light was collected by f/2 10 cm focal length lens and focused on the slit of a SPEX 1807 Triplemate operating as a spectrograph to disperse the light onto a Photometrics CCD camera. Typical data acquisition times were 40 min because of fluorescent backgrounds observed below the glass transition temperature. Above the glass transition temperature, acquisition times of 10 min sufficed to obtain spectra with a good signal-to-noise ratio.

Density Functional Theory Calculations

The density functional theory (DFT) calculations were performed using the MSI (Molecular Simulations, Inc.) ab initio quantum chemical software program DMol3.[24] DMol3 was used for geometry optimization, single-point energy, and frequency calculations of the substituted imidazole iron−porphine models designated Por(L), where Por and L represent the porphine and axial ligand, respectively. Comparisons of calculations of porphine−CO models with experimental results have been discussed elsewhere.[25,26] These calculations used the DNP basis set and the GGA functional in the gas phase. The graphical user interface InsightII (Accelerys, San Diego, CA) was used to build the models and to visualize the eigenvector projections calculated by DMol3. The DFT calculations were performed at the North Carolina Supercomputing Center (NCSC) on the IBM RS/6000 SP. Normal coordinate analysis was performed using FCART01[27] to calculate the potential energy distributions (PED) for the normal modes. The instrinic mode anharmoncities were determined by calculating potential energy surfaces (PES) along the iron−ligand out-of-plane normal mode formed by calculating the energy at displacements along the eigenvector from the optimized geometry. A fourth-order polynomial ($E(Q) = a_0 + a_1Q + a_2Q^2 + a_3Q^3 + a_4Q^4$) was used to fit the PES and these parameters were used in the Numerov−Cooley[28,29] method to calculate the energies and wave functions for the first five vibrational levels for this normal mode. The intrinsic mode anharmonicity was then calculated from the average energy (cm^{-1}) spacing difference between the first five adjacent vibrational levels (i.e., average difference between $\nu_0 - \nu_1$, $\nu_1 - \nu_2$, $\nu_2 - \nu_3$, $\nu_3 - \nu_4$). Anharmonic multimode coupling was investigated by projecting along the eigenvector of normal modes containing iron−axial out-of-plane motions (heme-doming) and calculating the shift in frequency in the iron−ligand out-of-plane normal mode relative to the equilibrium calculated frequency. The calculated shifts of the substituted imidazoles were normalized to imidazole by

$$\Delta\tilde{\nu}_{norm} = \left(\frac{PED_{Fe-N}(Im)}{PED_{Fe-N}(L)}\right)\left(\frac{MW(Im)}{MW(L)}\right) \quad (1)$$

where $\Delta\nu_{norm}$ is the normalized shift in the iron-ligand out-of-plane mode, PED is the potential energy distribution (% Fe−Nϵ stretching) of this mode, and MW is the molecular weight of imidazole (Im) or the substituted imidazole ligands (L) to account for the varying molecular weights and PED for the substituted imidazole ligands.

Results

The temperature dependence of the Raman spectra of H93G-(Im) and H93G(2-Me Im) are shown in Figures 1 and 2, respectively. A complete analysis of the spectra was carried out by fitting to multiple Gaussian bands to determine which bands shift as a function of temperature (see the Supporting Information). This analysis is essential because one interpretation of the multiple bands in the region from 190 to 240 cm^{-1} is that there are several conformations of the protein present.[14,30] However, a fit of this region to three to five independent Gaussians (depending on the ligand) yielded significant shifts from a single Gaussian band or a pair of Gaussians. The weighted mean frequency of these Gaussians showed a consistent trend to higher frequency and an increase in asymmetry as the temperature was lowered consistent with the anharmonic coupling model[17] (see the Supporting Information). To higher energy, the peaks at $\approx$263 and $\approx$283 cm^{-1} present in all of the Raman spectra do not show a consistent temperature-dependent shift. A nonshifting peak at $\approx$250 cm^{-1} appears in spectra of all adducts except 4-Br imidazole (data not shown). There is a nonshifting mode at $\approx$240 cm^{-1} in all of the adducts except

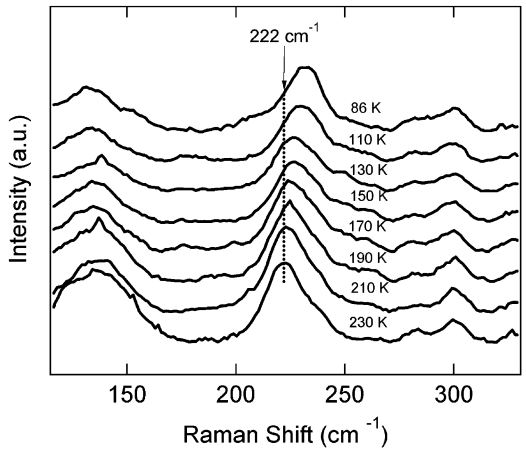

Figure 1. Temperature dependence of resonance Raman spectra of H93G(Im). The frequency shift of the iron-imidazole out-of-plane mode is shown relative to a dashed line at 230 K frequency of 222 cm^{-1}. Eight temperatures are shown from 86 to 230 K.

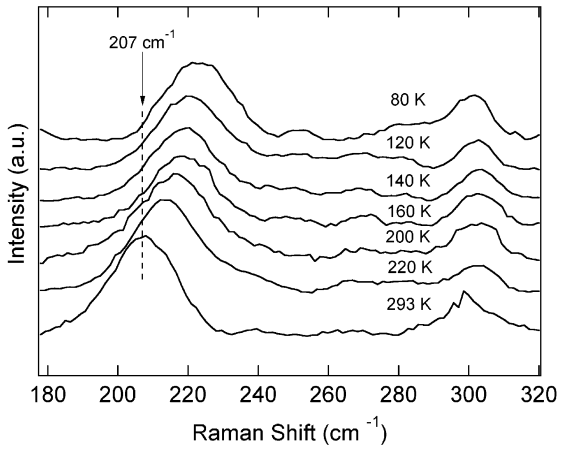

Figure 2. Temperature dependence of resonance Raman spectra of H93G(2-Me Im). The frequency shift of the iron-2-methyl-imidazole out-of-plane mode is shown relative to a dashed line at the room-temperature frequency of 207 cm^{-1}. Seven temperatures are shown from 80 to 293 K.

TABLE 1: Iron−Ligand Out-of-Plane Mode Frequency as a Function of Temperature for Axial Ligand Adducts to Deoxy Ferrous H93G Myoglobin

adduct	slope/100 K	100 K (cm^{-1})	293 K (cm^{-1})
4-Me Im	2.5 ± 0.3	223.2	218.7
horse heart	3.0 ± 0.2	223.0	217.7
1-Me Im	4.6 ± 0.2	238.6	229.2
imidazole	5.5 ± 0.3	230.6	220.6
4-Br−Im	5.9 ± 0.4	206.3	194.2
2,4-diMe Im	6.1 ± 0.4	206.7	194.5
2-Me Im	6.7 ± 0.5	221.0	207.1

H93G(2-Me Im). This band at ≈240 cm^{-1} is seen very clearly in both the horse heart and sperm whale myoglobin resonance Raman spectra and has been assigned as ν_9.[31] In each of the adducts of H93G myoglobin, there was a single Raman band that increased in frequency as the temperature was lowered from 293 to 83 K. The frequency shift for the temperature-dependent ν_{Fe-L} band for each of six adducts is reported in Table 1 along with that of wild-type horse heart myoglobin.

The H93G mutant can be prepared with no exogenous ligand present; however, the iron in this species is five coordinate with H_2O as the fifth ligand.[32] The Raman spectrum seen in Figure 3 has no iron−ligand out-of-plane mode in the region of the spectrum from 180 to 240 cm^{-1}. There is one pronounced

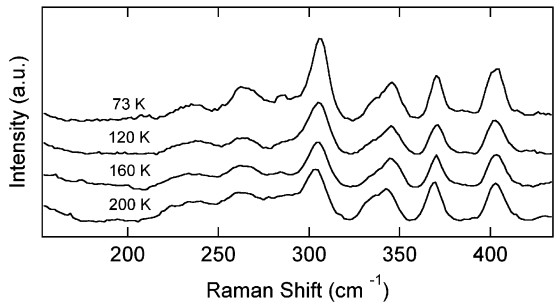

Figure 3. Temperature dependence of resonance Raman spectra of H93G with no exogenous ligand. There are no apparent shifts in the Raman bands below 320 cm^{-1} in these spectra. This suggests that all of the modes in this spectrum are heme modes that do not depend strongly on ligand identity. Four temperatures are shown from 73 to 200 K.

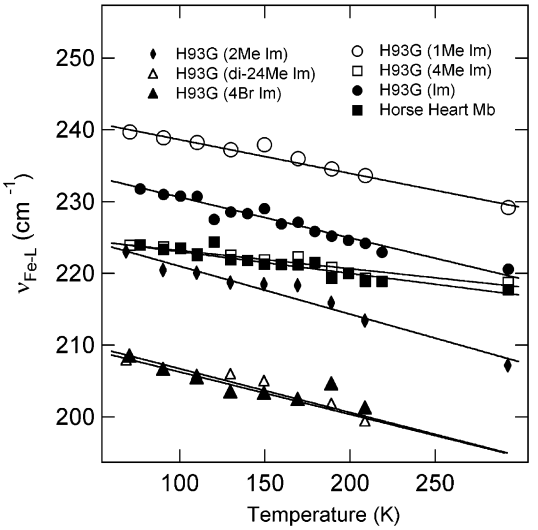

Figure 4. Dependence of the peak position of the iron−ligand out-of-plane mode on temperature. Plots of the peak positions of all of the iron-ligand modes studied in detail are shown. The data are fit to lines, and the slopes are presented in Table 1.

(nonshifting) peak in H93G(H_2O) at ≈236 cm^{-1} assigned as ν_9. The H93G(H_2O) species serves as a consistency test for the observation that only the band that corresponds to ν_{Fe-L} shifts with temperature. The vibrational modes seen in the spectrum of Figure 3 are nearly the same as the nonshifting modes seen in the spectra of the other H93G(L) ligand adducts. Consistent with the results for the imidazole adducts H93G(L), none of the bands in H93G(H_2O) show any temperature dependence.

The shift in the peak frequency of the iron−ligand out-of-plane mode for all of the ligands is plotted as a function of temperature in Figure 4. The peak shift was determined based on fits of all of the data to 3−5 Gaussians over the spectral range 190−240 cm^{-1}. The lines through the data points were obtained by a linear least-squares fit. The slopes and room-temperature values of the frequencies for each ligand are given in Table 1. Comparing the slopes given in Table 1 shows that ν_{Fe-L} for H93G(2-Me Im) has a temperature dependence more than twice as large as that of either wild-type horse heart myoglobin or H93G(4-Me Im). The H93G(1-Me Im) adduct studied consisted of the di-^{15}N isotopomer. The isotopomer of 1-Me Im was used because the Raman spectrum for H93G(1-Me Im) shows a Fermi resonance that would obscure the frequency shifts reported.[23] H93G(1-Me Im) also shows a frequency shift twice as large as that of H93G(4-Me Im). This result is surprising because the structures of 4-Me Im and 1-Me Im are quite similar in the proximal pocket.[33]

TABLE 2: Iron-Ligand Out-of-Plane Mode DFT Calculated Frequencies, Potential Energy Distributions, and Intrinsic Mode Anharmonicities

adduct	Fe−Nϵ distance (Å)	Fe−Nϵ binding energy (kJ/mol)[a]	ν_{Fe-L} (cm^{-1})	PED Fe−Nϵ stretch	$\|\Delta\tilde{\nu}\|$ single mode (cm^{-1})[b]	doming mode (cm^{-1})[c]	$\|\Delta\tilde{\nu}\|$ multimode (cm^{-1})[d]
4-Me Im	2.19	75.2	143.2	44%	(+)0.3	76.8	0.4
1-Me Im	2.16	75.3	160.5	73%	(−)0.3	80.9	5.1
imidazole	2.18	74.0	169.9	66%	(−)0.2	87.3	1.0
4-Br Im	2.19	70.4	142.9	64%	(+)0.1	70.3	3.3
2,4-diMe Im	2.20	78.6	155.5	55%	(+)3.2	84.2	3.7
2-Me Im	2.21	74.8	163.0	61%	0.0	74.8	3.8

[a] Binding energy = $(Fe-N\epsilon)_{10\ Å} - (Fe-N\epsilon)_{equilibrium\ distance}$ [b] Average anharmonicty over first five vibrational levels. (−) Decrease in energy spacing; (+) increase in energy spacing going up in vibrational levels. [c] Energy of the low wavenumber heme-doming normal mode that was displaced by 0.5 normal coordinate units along its eigenvector projection. [d] Normalized shift ($\Delta\tilde{\nu}$) in the iron−ligand out-of-plane mode of the substituted imidazole ligands to imidazole to account for the different molecular weights and % Fe−Nϵ stretching of the iron−ligand out-of-plane mode as shown above.

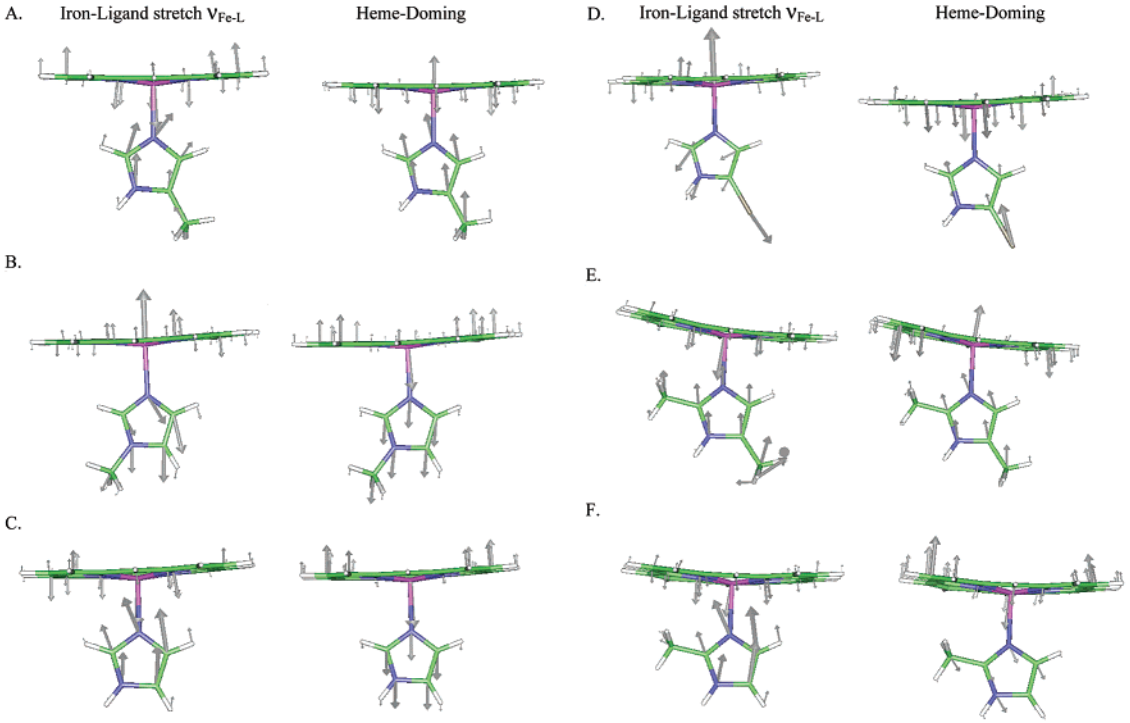

Figure 5. DFT calculated eigenvector projections of the iron−ligand out-of-plane mode, ν_{Fe-L}, and the heme-doming mode for the porphine models. 4-Me Im (A), 1-Me Im (B), imidazole (C), 4-Br Im (D), 2,4-diMe Im (E), and 2-Me Im (F).

The vibrational spectrum of each adduct within the harmonic approximation was obtained by finite difference based on the energies of a DFT calculation for a model complex that consisted of an iron porphine with an axial ligand. Table 2 gives the calculated equilibrium distances, binding energies, and frequencies of the Fe−Nϵ bond for the various substituted porphine models with axial imidazole ligands. The mode identified as ν_{Fe-L} from the calculation, i.e., the mode that shows the greatest PED for the Fe−Nϵ stretching coordinate, is found in the wavenumber range from 140 to 170 cm^{-1} for all model adducts as shown in Table 2. Consistent with a previous analysis,[23] the Fe−Nϵ stretching component of the iron−ligand out-of-plane mode is between 44 and 73% for the porphine adducts. However, the calculated frequencies for ν_{Fe-L} are on average ≈27% lower than the corresponding observed Raman frequencies given in Table 1. This difference is somewhat surprising because DFT calculations of high-frequency modes in metalloporphines tend to be much more accurate.[25,26,34,35] The mode calculated in the 228−239 cm^{-1} mode, i.e., closest to the experimentally observed frequency, is predominantly an iron out-of-plane motion that has little Fe−Nϵ stretching character.

In addition to the contribution of the internal coordinates to the vibrational modes within the harmonic approximation, anharmonic coupling of a low-frequency heme-doming mode with the iron−ligand out-of-plane mode has been proposed based on a two-mode quantum mechanical model.[17] The eigenvectors obtained from DFT calculations shown in Figure 5 correspond to a heme-doming mode that ranges from 70 to 90 cm^{-1} in the various adducts as given in Table 2. The value of 70−90 cm^{-1} calculated here for the iron-doming mode is in the range of 50−100 cm^{-1} found for previous calculations[41,42] and experiments.[43] On the basis of the PED, we have performed the analysis of anharmonicity using the 130−160 cm^{-1} as the model for the ν_{Fe-L} mode including both the intrinsic anharmonicity and anharmonic coupling to the low wavenumber heme-doming mode. The intrinsic anharmonicity of the iron−ligand mode was calculated using potential energy surfaces derived from projections along the eigenvectors shown in Figure 5. The corresponding PES of the iron−ligand mode for each of the substituted imidazole-porphine models with the first five vibrational wave functions calculated using the Numerov−Cooley method is shown in the Supporting Information. The

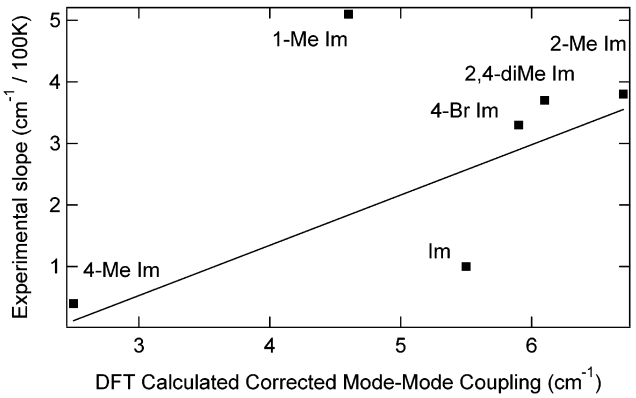

Figure 6. Plot of the iron−ligand out-of-plane frequency temperature dependence versus the DFT calculated normalized intermode anharmonic coupling between the low-frequency heme-doming mode and the iron−ligand out-of-plane mode for the substituted imidazole ligands.

intrinsic cubic anharmonicities were calculated to be less than 0.5 cm^{-1} for the substituted imidazole ligands. The Por(2,4-diMe Im) calculation showed a relatively large quartic anharmonicity (3.0 cm^{-1}).

Anharmonic multimode coupling of the heme-doming and iron−ligand out-of-plane mode was studied by displacing along the normal mode (eigenvector) of low wavenumber heme-doming mode and calculating the resulting shift in the calculated frequency of the ν_{Fe-L} mode. The heme-doming modes (Figure 5) were calculated to be 70−90 cm^{-1} and were displaced by 0.5 mass-weighted normal coordinate units[36] to calculate the relative magnitude of anharmonic multimode coupling for the various imidazole ligands. Table 2 shows the calculated shifts that were normalized (eq 1) to take into account the different masses and percentages of Fe−Nϵ stretching motion in the iron−ligand out-of-plane mode for the substituted imidazole ligands (see also the Supporting Information). Figure 6 shows the linear dependence of the slope of the experimental Raman temperature dependence of the iron−ligand out-of-plane mode (Table 1) and the DFT calculated normalized intermode anharmonic coupling between the low-frequency heme-doming mode and ν_{Fe-L} (Table 2). This plot illustrates that the calculated normalized shifts parallel the experimental data, with the exception of the model porphine adduct of 1-Me Im. The ordering of the magnitude of the shifts is Por(2-Me Im) > Por(2,4-diMe Im) > Por(4-Br Im) > Por(Im) > Por(4-Me Im) in agreement with experiment as seen by comparing Tables 1 and 2. Although the Im ligand lies below the correlation line in Figure 6, it follows the ordering of anharmonicities. The magnitude of the calculated shift is arbitrary in the current model. It is dependent on the magnitude of the displacement in the anharmonically coupled heme-doming mode. To obtain a quantitative comparison, displacement along a number of coordinates must be carried out combined with vibrational frequency calculations at each displacement. The shift can be calculated as the expectation value of the frequency shift (harmonic shift approximation) as discussed elsewhere.[36] Several other possible modes were investigated that could potentially give rise to anharmonic coupling (see the Supporting Information).

Discussion

Despite a large number of studies of the iron−histidine resonant Raman band in heme proteins, there have been relatively few studies of the temperature dependence of the ν_{Fe-His} vibrational mode in native heme proteins.[6,14,15,37,38] The results for various ligands in H93G(L) suggest that the temperature dependences can be substantial. This appears to be particularly true for the iron adduct of the hindered ligand 2-methyl imidazole. The H93G(2-Me Im) adduct is interesting because it was used in the first heme models used to assign the iron−histidine stretch.[2,39] The 2-methyl imidazole adduct of heme has also been interpreted as a model for T-state hemoglobin.[2] We have recently shown that photolyzed H93G(2-Me Im)CO shows a large shift in the ν_{Fe-L} band in the 8 ns photoproduct analogous to the photolyzed R-state of HbCO.[40] This comparison is further substantiated in the present data because both T-state hemoglobin and H93G(2-Me Im) appear to have a relatively large temperature dependence of their ν_{Fe-His} bands.[15] On the other hand, the temperature dependence of ν_{Fe-L} in H93G(4-Me Im) is nearly identical to that of horse heart myoglobin consistent with the fact that 4-Me Im is chemically most closely related to imidazole of all of the ligands that can be substituted into H93G. It is interesting that H93G(4-Me Im) and H93G(2-Me Im) represent the smallest and largest temperature dependence, respectively.

The calculated value for the shift of ν_{Fe-L} of H93G(1-Me Im) due to anharmonic coupling does not follow the trend of the other ligands. The ν_{Fe-L} Raman band for the natural abundance isotopomer of H93G(1-Me Im) is the only one that shows a Fermi resonance.[23] The dideutero isotopomer of 1-Me Im removes the splitting of the Fermi resonance; however, the DFT calculation corresponds to the natural abundance isotopomer. The Fermi resonance of H93G(1-Me Im) indicates that anharmonic coupling to modes other than the heme doming is likely present for 1-Me Im. Therefore, the anharmonic coupling model applied to the DFT calculation does not necessarily account for the true anharmonic coupling present in H93G(1-Me Im). The difference in anharmonic coupling is remarkable because the structures of H93G(1-Me Im) and H93G(4-Me Im) have been shown to be nearly identical by X-ray crystallography.[33] However, 1-Me Im and 4-Me Im differ in their hydrogen bonding because 4-Me Im can form strong a H bond with serine 92, whereas 1-Me Im cannot. In fact, the 1-Me Im adduct is the only substituted imidazole that is incapable of hydrogen bonding. Although the link between this observation and the spectral anomalies has not yet been established, these facts do suggest that H93G(1-Me Im) should be considered separately from the other ligands.

The DFT calculations suggest that intrinsic (single-mode) mode anharmonicity of the iron−ligand out-of-plane mode does not explain the observed frequency shifts of this band in the temperature dependent Raman spectra. On the other hand, anharmonic coupling of a low-frequency heme-doming mode with the iron−ligand stretch (intermode coupling) does account relatively well for the data. The success of this calculated model verifies conclusions obtained previously using a two-mode quantum mechanical model.[17] Moreover, the calculation suggests that additional effects due to off-axis tilting are small relative to the iron-doming mode contribution to anharmonic coupling.

The data obtained in the present study can be compared with 8 ns photoproduct spectra obtained on some of the same ligands. The relative magnitude of shifts in the ν_{Fe-L} mode is quite different in that case. The ordering of the photoproduct shifts in 75% glycerol/buffer is H93G(2-Me Im) > H93G(4-Me Im) > H93G(1-Me Im) = H93G(Im). The origin of shifts in the photoproduct spectra does not appear to depend on the anharmonic coupling to the iron-doming mode.

The present study supports interpretations of the frequency in terms of bonding and strain that have been advanced in a range of heme proteins.[7] Moreover, the success of the anhar-

monic coupling model strongly suggests that the apparent non-Gaussian line shape of the ν_{Fe-L} Raman band arises from the presence of Raman bands from modes that are not anharmonically shifted rather than conformational substates of myoglobin.[14,44] The A-states of myoglobin are observed in the CO-bound form as multiple infrared CO stretching bands.[45−47] The B states of myoglobin are observed in the photoproduct, i.e., when the CO ligand is still present in the protein but not bound to the heme iron.[48−50] Although it is logical to seek conformational substates with barriers of similar height in the deoxy form, the present study suggests that the ν_{Fe-L} Raman band does not provide evidence for such conformational substates in deoxy myoglobin.

Conclusions

Temperature-dependent Raman frequency shifts of the iron−ligand out-of-plane mode, ν_{Fe-L}, have been observed for a variety of substituted imidazole ligands in the H93G mutant of myoglobin. The magnitude of the frequency shift was dependent on the identity of the substituted imidazole ligand present and decreased in the order H93G(2-Me Im) > H93G(2,4-diMe Im) > H93G (4-Br Im) > H93G (Im) > H93G(1-Me Im) > H93G-(4-Me Im). With the exception of the H93G(1-Me Im) adduct, the trend is the same as that calculated using an anharmonic intermode coupling by DFT methods. DFT calculations support earlier suggestions that this normal mode had a significant (44−73%) component of Fe−Nϵ stretching motion; however, the calculated frequency of the ν_{Fe-L} mode is substantially lower than the observed mode frequency. The DFT calculations are consistent with a doming mode at lower frequency than the ν_{Fe-L} mode that is strongly anharmonically coupled to the ν_{Fe-L} mode. These observations corroborate the results of other studies both regarding the PED of the ν_{Fe-His} mode[23,51] and the frequency of the doming[41,42] as well as its anharmonic coupling.[17] The success of an intermode anharmonic coupling model is a significant step both in the field of heme protein spectroscopy and in the development of DFT methods for the analysis of spectroscopy.

Acknowledgment. S.F. acknowledges a Director's Fellowship at Los Alamos National Laboratory. Raman data were obtained at Los Alamos National Laboratory. S.F. acknowledges support by NSF Grant MCB-9874895. S.B. was supported by the NIH Biotechnology Training Grant T32-GM08776. We thank S. Stavrov for helpful discussions. S.F. and S.B. acknowledge support by the North Carolina Supercomputer Center (NCSC).

Supporting Information Available: A complete analysis of the spectra. This material is available free of charge via the Internet at http://pubs.acs.org.

References and Notes

(1) Argade, P. V.; Sassaroli, M.; Rousseau, D. L.; Inubushi, T.; Ikeda-Saito, M.; Lapidot, A. *J. Am. Chem. Soc.* **1984**, *106*, 6593−6596.
(2) Nagai, K.; Kitagawa, T.; Morimoto, H. *J. Mol. Biol.* **1980**, *136*, 271−289.
(3) Scott, T. W.; Friedman, J. M. *J. Am. Chem. Soc.* **1984**, *106*, 5677−5687.
(4) Sage, J. T.; Morikis, D.; Champion, P. M. *Biochemistry* **1991**, *30*, 1227−1237.
(5) Matsukawa, S.; Mawatari, K.; Yoneyama, Y.; Kitagawa, T. *J. Am. Chem. Soc.* **1985**, *107*, 1108−1113.
(6) Ahmed, A. M.; Campbell, B. F.; Caruso, D.; Chance, M. R.; Chavez, M. D.; Courtney, S. H.; Friedman, J. M.; Iben, I. E. T.; Ondrias, M. R.; Yang, M. *Chem. Phys.* **1991**, *158*, 329−351.
(7) Spiro, T. G.; Smulevich, G.; Su, C. *Biochemistry* **1990**, *29*, 4497−4508.
(8) Woodruff, W. H.; Einarsdottir, O.; Dyer, R. B.; Bagley, K. A.; Palmer, G.; Atherton, S. J.; Goldbeck, R. A.; Dawes, T. D.; Kliger, D. S. *Proc. Natl. Acad. Sci.* **1991**, *88*, 2588−2592.
(9) Goodin, D. B.; McRee, D. E. *Biochemistry* **1993**, *32*, 3313−3324.
(10) Argade, P. V.; Ching, Y. C.; Rousseau, D. L. *Science* **1984**, *255*, 329−331.
(11) Tsukihara, T.; Aoyama, H.; Yamashita, E.; Tomizaki, T.; Yamaguchi, H.; Shinzawa-Itoh, K.; Nakashima, R.; Yaono, R.; Yoshikawa, S. *Science* **1995**, *269*, 1069−1074.
(12) Franzen, S.; Dyer, R. B.; Woodruff, W. H.; Roach, M. R.; Chen, Y. P.; Dawson, J. H. *J. Am. Chem. Soc.* **1998**, *120*, 4658−4661.
(13) Schelvis, J. P. M.; Kim, S. Y.; Zhao, Y. D.; Marletta, M. A.; Babcock, G. T. *J. Am. Chem. Soc.* **1999**, *121*, 7397−7400.
(14) Gilch, H.; Schweitzer-Stenner, R.; Dreybrodt, W. *Biophys. J.* **1993**, *65*, 1470−1485.
(15) Ondrias, M. R.; Friedman, J. M.; Rousseau, D. L. *Science* **1983**, *220*, 615−617.
(16) The ν_{Fe-His} band is cited as having a frequency of 218−220 cm^{-1}. The frequency quoted here is 75% glycerol/buffer solution which gives rise to a shift to lower wavenumer by 2 cm^{-1}.
(17) Rosenfeld, Y. B.; Stavrov, S. S. *Chem. Phys. Lett.* **1994**, *229*, 457−464.
(18) Barrick, D. *Biochemistry* **1994**, *33*, 6546−6554.
(19) DePillis, G.; Decatur, S. M.; Barrick, D.; Boxer, S. G. *J. Am. Chem. Soc.* **1994**, *116*, 6981−6982.
(20) Desbois, A.; Lutz, M. *Biochim. Biophys. Acta* **1981**, *671*, 168−176.
(21) Collman, J. P. *Acc. Chem. Res.* **1977**, *10*, 265−272.
(22) Geibel, J.; Cannon, J.; Campbell, D.; Traylor, T. G. *J. Am. Chem. Soc.* **1978**, *100*, 3575−3585.
(23) Franzen, S.; Boxer, S. G.; Dyer, R. B.; Woodruff, W. H. *J. Phys. Chem. B* **2000**, *104*, 10359−10367.
(24) Delley, B. *J. Chem. Phys.* **1990**, *92*, 508−517.
(25) Franzen, S. *J. Am. Chem. Soc.* **2001**, *123*, 12578−12589.
(26) Franzen, S. *J. Am. Chem. Soc.* Submitted.
(27) Collier, W. B. *QCPE Bull.* **1993**, *13*, 19.
(28) Cashion, J. K. *J. Chem. Phys.* **1963**, *39*, 1872−1877.
(29) Eccles, J.; Malik, D. *QCPE Bull.* **1981**, *13*, 407.
(30) Gilch, H.; SchweitzerStenner, R.; Dreybrodt, W.; Leone, M.; Cupane, A.; Cordone, L. *Int. J. Quantum Chem.* **1996**, *59*, 301−313.
(31) Hu, S.; Smith, K. M.; Spiro, T. G. *J. Am. Chem. Soc.* **1996**, *118*, 12638−12646.
(32) Franzen, S.; Bailey, J.; Dyer, R. B.; Woodruff, W. H.; Hu, R. B.; Thomas, M. R.; Boxer, S. G. *Biochemistry* **2001**, *40*, 5299−5305.
(33) Barrick, D.; Dahlquist, F. W. *Proteins: Struct., Funct., Genet.* **2000**, *39*, 278−290.
(34) Vogel, K. M.; Kozlowski, P. M.; Zgierski, M. Z.; Spiro, T. G. *Inorg. Chim. Acta* **2000**, *297*, 11−17.
(35) Vogel, K. M.; Kozlowski, P. M.; Zgierski, M. Z.; Spiro, T. G. *J. Am. Chem. Soc.* **1999**, *121*, 9915−9921.
(36) Lappi, S. E.; Collier, W.; Franzen, S. *J. Phys. Chem.* Submitted.
(37) Rousseau, D. L.; Argade, P. V. *Proc. Natl. Acad. Sci. U.S.A.* **1986**, *83*, 1310−1314.
(38) Sassaroli, M.; Rousseau, D. L. *Biochemistry* **1987**, *26*, 3092−3098.
(39) Hori, H.; Kitagawa, T. *J. Am. Chem. Soc.* **1980**, *102*, 3608−3613.
(40) Franzen, S.; Peterson, E. S.; Brown, D. A.; Thomas, M. R.; Friedman, J. M.; Boxer, S. G. *Eur. J. Biochem.* Submitted.
(41) Li, X.-Y.; Zgierski, M. Z. *Chem. Phys. Lett.* **1992**, *188*, 16−20.
(42) Li, P.; Sage, J. T.; Champion, P. M. *J. Chem. Phys.* **1992**, *97*, 3214−3227.
(43) Sage, J. T.; Paxson, C.; Wyllie, G. R. A.; Sturhahn, W.; Durbin, S. M.; Champion, P. M.; Alp, E. E.; Scheidt, W. R. *J. Phys. Condens. Matter* **2001**, *13*, 7707−7722.
(44) Schott, J.; Dreybrodt, W.; Schweitzer-Stenner, R. *Biophys. J.* **2001**, *81*, 1624−1631.
(45) Frauenfelder, H.; Park, F.; Young, R. D. *Annu. Rev. Biophys. Chem.* **1988**, *17*, 451−479.
(46) Caughey, W. S.; Alben, J. O.; McCoy, S.; Boyer, S. H.; Carache, S.; Hathaway, P. *Biochemistry* **1969**, *8*, 59−62.
(47) Potter, W. T.; Hazzard, J. H.; Choc, M. G.; Tucker, M. P.; Caughey, W. S. *Biochemistry* **1990**, *29*, 6283−6295.
(48) Alben, J. O.; Beece, D.; Bowne, S. F.; Doster, W.; Eisenstein, L.; Frauenfelder, H.; Good, D.; McDonald, J. D.; Marden, M. C.; Moh, P. P.; Reinisch, L.; Reynolds, A. H.; Shyamsunder, E.; Yue, K. T. *Proc. Natl. Acad. Sci.* **1982**, *79*, 3744−3748.
(49) Lim, M.; Jackson, T. A.; Anfinrud, P. A. *J. Chem. Phys.* **1995**, *102*, 4355−4366.
(50) Lim, M. H.; Jackson, T. A.; Anfinrud, P. A. *Nat. Struct. Biol.* **1997**, *4*, 209−214.
(51) Wells, A. V.; Sage, T. J.; Morikis, D.; Champion, P. M.; Chiu, M. L.; Sligar, S. G. *J. Am. Chem. Soc.* **1991**, *113*, 9655−9660.